

Computational Fluid Dynamics Investigation of Air-Gas Pre Mixing Controller Mixer Designed for CNG-Diesel Dual-Fuel Engines


 Open
Access

 Hassan Sadah Muhssen^{1, 2, *}, Siti Ujila Masuri¹, Barkawi Sahari¹, Abdul Aziz Hairuddin¹
¹ Department of Mechanical and Manufacturing Engineering, Faculty of Engineering, Universiti Putra Malaysia, 43400 UPM Serdang, Selangor, Malaysia

² Department of Mechanical Engineering, University of Wasit, Wasit, Iraq

ARTICLE INFO
ABSTRACT
Article history:

Received 18 April 2019

Received in revised form 25 May 2019

Accepted 2 June 2019

Available online 3 July 2019

CNG-air mixer is a device like carburetor that used to convert the diesel engine to dual fuel engine without more engine modifications. The main purpose of this mixer is to supply the engine by homogeneous CNG-air mixture simultaneously with suitable air-fuel ratios (AFR_s) as required by the engine. The best mixing of gas and air is hardly achieved due to stationary parts of existing types of mixer. Therefore, this paper carried out a computational fluid dynamics (CFD) study to investigate the performance of new commercial mixer. This mixer is a secondary fuel pre mixing controller designed for a 3.168 liter dual fuel-diesel engine and positioned at the air inlet manifold. The mixing process of CNG and air is controlled by the interior design of the mixer and the movement of controller valve. Preliminary analysis was conducted when the maximum engine speed (3600 rpm) and at a fully open secondary fuel inlet pipe. With this case, atmospheric pressure was used at the gas inlet to see if the gas could be sucked or need to be supplied with pressure higher than atmospheric pressure. The second step of investigation was done when the valve moved to last position and mass flowrate was used at the mixer outlet and gas inlet according to required air fuel ratio (AFR) to find the pressure at the gas inlet besides examine the homogeneity of CNG-air mixture. The mixer had been tested with various AFR_s starting with (10) for rich, (17.2) for stoichiometric, and (20, 30, 40) for lean combustion. Uniformity index (UI) and color contours of methane mass fraction (M_{CH₄}) were used to evaluate the mixing quality of CNG and air. The results of testing showed that the gas should be supplied with pressure higher than atmospheric pressure to obtain the AFR close to stoichiometric ratio. This pressure was very high which not allowed in the pressure regulator that available in the market. This problem caused by the design of control valve shaft. Furthermore, the study showed that the mixer is unable to provide a homogeneous mixture of CNG and air. Therefore, the mixer needs to be optimized in terms of controlling AFR and CNG-air mixture homogeneity.

Keywords:

CNG-air mixer; computational fluid dynamics; dual-fuel systems

Copyright © 2019 PENERBIT AKADEMIA BARU - All rights reserved

* Corresponding author.

 E-mail address: hassan.wassit@yahoo.com, hassan.kut85@yahoo.com (Hassan Sadah Muhssen)

1. Introduction

High thermal efficiency, durability, low carbon dioxide emission, reliability, high torque, and fuel economy are the factors that made the diesel engines preferable to passenger transport, trucks, and power generation operations. In contrast, high localized temperature and combustion with heterogeneous air-fuel mixture have made the diesel engine produces a high level of nitrogen oxides emission and particulate matter emission [1-3]. Previous investigations showed that people are prone to heart and lung diseases when exposed to exhaust particulate matter emission [1, 4]. Many types of alternative fuels like alcohol, CNG, LPG, biogas, producer gas, and hydrogen were studied broadly in the literature [5]. The factors such as high auto-ignition temperature, clean nature of combustion, and high availability at attractive prices make the natural gas as a good alternative fuel for diesel and gasoline engines [6-8].

Compressed natural gas (CNG) is one of the of natural gas forms, which has some properties made it as attractive alternative fuel for diesel fuel such as high octane ratio, high hydrogen to carbon rate, and leaner burn due to wide ignition limit [8, 9]. Although the significant role of CNG in reducing combustion emissions, the problem of high rate of NO_x and PM (particulate matter) emissions has been taken into account in recent times [7, 10-13]. CNG-diesel dual fuel (DDF) system has been developed to decrease NO_x and particulate emissions of diesel engines [1, 12, 14-16]. The working principle of dual-fuel IC engine is represented by burning amount of the premixed gaseous fuel-air mixture by injecting a small amount of diesel fuel into the engine combustion chamber near the end of the compression stroke [17, 18].

CNG-air mixer is a device like carburetor that positioned at the air intake manifold and used to convert the diesel engine to dual fuel engine without more engine modifications [11, 19-23]. The main purpose of the mixer is to obtain a homogeneous mixture and suitable ratios of air and CNG as required by the engine [8, 22, 24-27]. Performances of the DDF engines in terms of power output and exhaust gas emissions are related to the combustion efficiency. Better performance of the DDF engines can be obtained if the mixture of air and CNG is homogeneously mixed prior to entry to the combustion chamber [8, 19, 23, 26, 28, 29].

Previous works proved that by an application of mixing chamber such as a CNG-air mixer, there is no losses occur in terms of power output at higher engine speeds due to the CNG fuel starvation [30, 31]. Besides that, power output and efficiency of the diesel-dual fuel engines are also affected by the amount of air induced to combustion chamber. The reduction of air quantity induced leads to a drop in engine power and efficiency. Therefore, the diesel-dual fuel engine should not to be throttled on the air side [32]. Throttle body injection mixer, venturi mixer, high-pressure mixer, venturi mixjector, intake manifold CNG injector, and secondary fuel premixing controller are the devices used to mix the CNG and air prior to entering the engine combustion chamber [11, 19-23].

All these mixing devices have been investigated deeply except the latter type, secondary fuel premixing controller. The best mixing of gas and air is hardly achieved due to stationary parts of existing types of mixer. Consequently, this study focused on the modeling and performance investigation of the secondary fuel premixing controller in terms of flow behavior and mixing quality of CNG-Air mixture.

2. Design of CNG-Air Mixer

The mixer which modeled and investigated in the present work is a secondary fuel premixing controller as shown in Figure 1. Ansys Design Modeler and CATIA were the software that used for modeling the mixer while the Ansys Fluent was used for analysis. This mixer contains a hollow casing

including an air inlet, a CNG-air mixture outlet, the main controller body, spring, and control valve connected together in central grouping one to another. The air passes through the mixer air inlet and pushes the control valve to open the pathway of air and CNG, and then the CNG-air mixture passes through the mixer outlet to the engine manifold. The main controlling body contains the housing which supports the axial movement of a control valve and contains the CNG fuel manifold which consists of gas entrance, gas distribution room, and the asymmetrical distribution space seven gas outlet holes. These holes positioned with air streamline as shown in Figures 1 and 2. The working principle of this mixer is represented by fixing the inlet pressure of CNG, while the amount of CNG is controlled by the surface design of control valve shaft which open and close the CNG pathway during the movement of control valve as shown in Figure 1. The flow pattern of CNG and air is shown in Figure 2. The control valve is biased to open and close the inner end of the CNG inlet according to the engine air-fuel requirement.

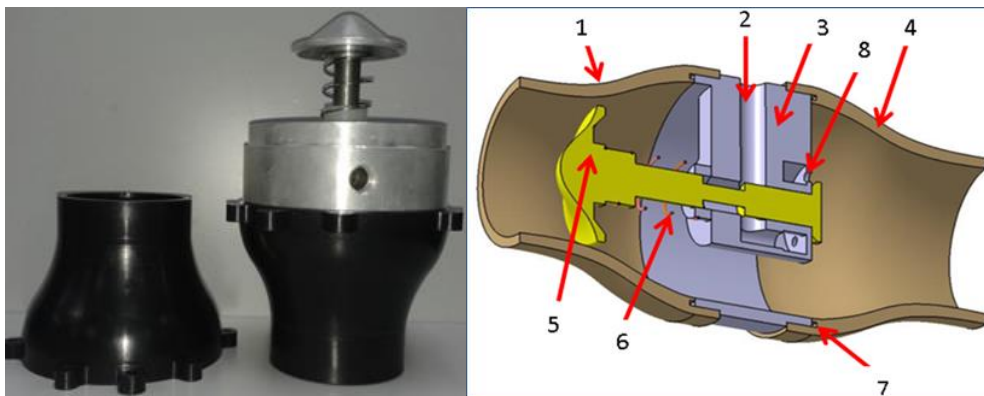


Fig. 1. Parts of secondary fuel pre mixing controller. 1- Air inlet part, 2- CNG entrance, 3- Main controller body, 4- Mixture outlet part, 5- Control valve, 6- spring, 7- Plastic washer, 8-CNG outlet holes

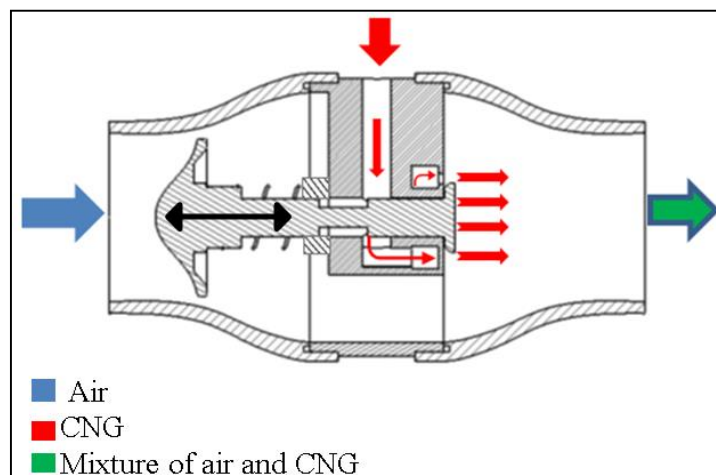


Fig. 2. Boundary inputs and outputs for the mixer

3. Numerical Setup

In order to obtain accurate results from simulation software, verification, and mesh independent test were used before doing any test for the mixer.

3.1 Verification

In this research, verification is represented by repeating experimental work by CFD software and found the error rate between experimental and CFD results. This process has been used to confirm that the CFD software is working properly, in addition, to make a sure that the collected boundary conditions and solving methods give results close to experimental results. Out of all research about CNG-air mixer, thesis done by Ramasamy. [33] to develop a CNG-air mixer for a two-stroke internal combustion engine was used in this verification because the researcher mentioned all mixer dimensions and boundary conditions. Figure 3 shows the best fit drawn lines of pressure drop points for each engine speed to indicate the errors between Ramasamy’s [33] experiments and the current simulation results. A maximum of 4.52% pressure drop error on an average of all points was found between Ramasamy’s [33] experiment and current simulation results, while for Ramasamy’s [33] experiment and simulation results the pressure drop error was 4.96%.

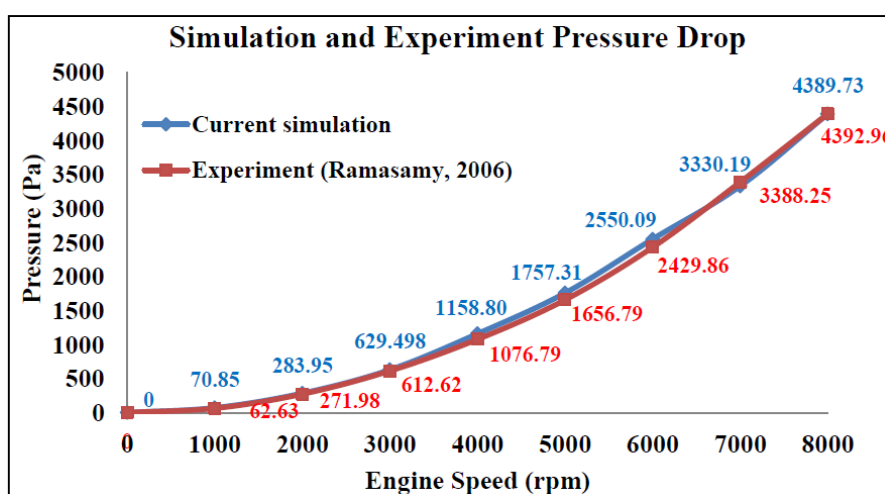


Fig. 3. New simulations and experiment pressure drop results along CNG-air mixer with various engine speeds

3.2 Mesh Generation

Mesh means to divide the solid or fluid geometry into finite volume cells consists of nodes and faces. The quality of mesh is very important since the computational fluid dynamics equations like momentum, energy, continuity, turbulent, and species transport are solved in these finite volume mesh cells. Unstructured tetrahedral independent mesh method was used for the fluid part of the mixer using ANSYS ICEM CFD mesh. Before further simulation was done a mesh dependence test was carried in order to ensure that the results are not affected by increasing the number of mesh cells. The mesh was gradually increased from mesh 1 to mesh 2, mesh 3, mesh 4, mesh 5 and mesh 6 as shown in Table 1 and Figure 4. The testing results show that a rough grid, i.e., mesh 1, which consists of 269937 cells, is the only mesh giving a little different result of M_{Ch4} and pressure as seen in Figure 5 and Figure 6. The other meshes show very close results of M_{Ch4} and pressure as seen in Figure 5 and Figure 6. Based on these tests, mesh consists of 505872 grid cells, was selected because less CPU time was spent for calculation. In addition to mesh dependence test, care was taken to minimize the maximum skewness which should not exceed 95%.

Table 1
 Number of cells for each level for original mixer simulation

Mesh Level	Mesh 1	Mesh 2	Mesh 3	Mesh 4	Mesh 5	Mesh 6
Fluid Elements Number	269937	390141	465899	505872	631673	1020032

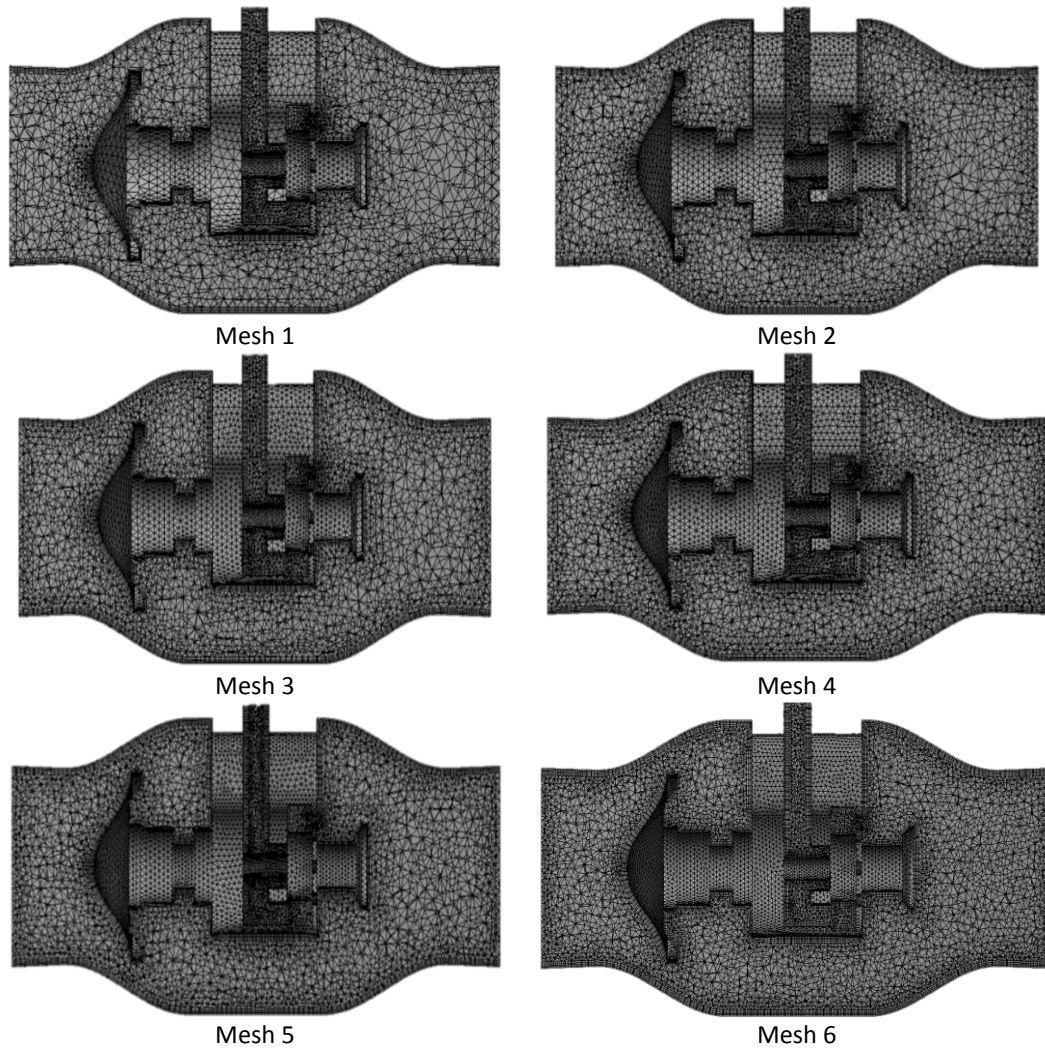


Fig. 4. Mesh Levels analyzed

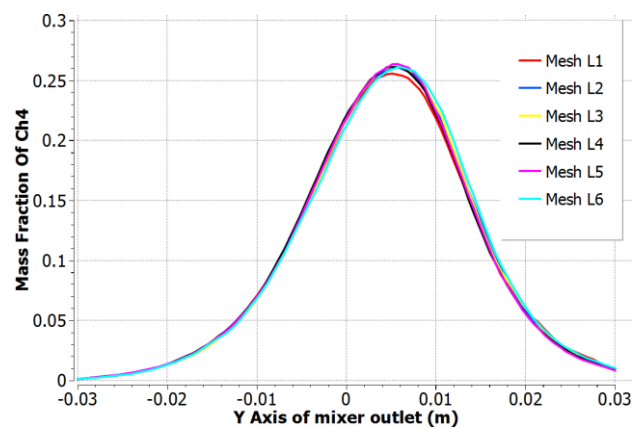


Fig. 5. Methane mass fraction on the line (vertical diameter) at the outlet of original mixer for different mesh elements

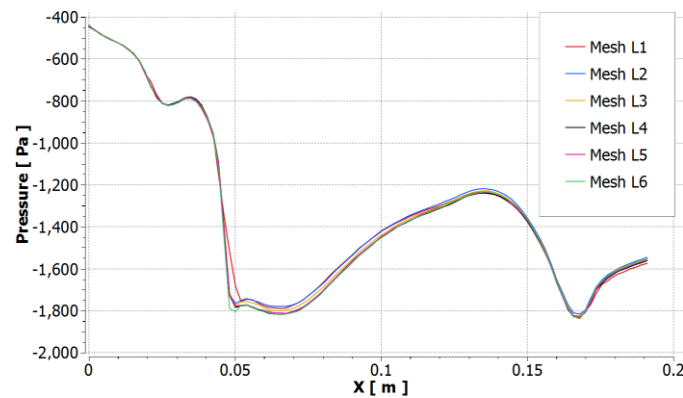


Fig. 6. Static pressure on the line (parallel to mixer axis) along the mixer for different mesh elements

3.3 Models and Boundary Conditions

When a specific mesh was reached for the mixer, suitable solution methods, solver, models, boundary conditions, controls, and monitors were chosen in the CFD software to begin the calculations.

3.3.1 Solver

Pressure-based solver and density-based solver are two available numerical methods in ANSYS FLUENT to choose one of them for solving.

The pressure-based approach was used in this work because it developed for low-speed incompressible flows while the density-based approach was mainly used for high-speed compressible flows. ANSYS FLUENT 14.5 provides four segregated types of algorithms: SIMPLEC, SIMPLE, PISO, and (Non-Iterative Time Advancement option (NITA) for time-dependent flows) Fractional Step (FSM). SIMPLE (Semi-implicit method for pressure link equation) method was used in this work as the solution algorithm. The SIMPLE method was chosen because it is used solely for steady state calculations in the iterative mode [34, 35]. For tetrahedral and triangular meshes, since the flow is never aligned with the mesh, mostly more accurate results obtain by using the second-order discretization. For hex/quad meshes, better results obtain by using the second order discretization, especially for complex flows. In brief, while the first-order discretization mostly yields better convergence than the second-order scheme, it generally yields less accurate results, especially on triangular/tetrahedral meshes [36].

3.3.2 Models

3.3.2.1 Energy equation

Since the simulation deals with species transport, energy equation was activated [36].

3.3.2.2 Turbulent model

The fluid flow was assumed as a turbulent flow according to high Reynolds number which obtained from Eq. 1 [37, 38].

$$Re = \frac{\rho v x}{\mu} \quad (1)$$

where R_e is Reynolds number, ρ and μ are the fluid density and viscosity respectively, and x is the characteristic length (pipe diameter).

The turbulent model which used in this study among wholly turbulent models is the κ - ϵ model because it is well validated and extensively used for fluid flow [19, 24, 39, 40]. K is the turbulence kinetic energy and is defined as the variance of the fluctuations in velocity and ϵ is the turbulence eddy dissipation [24, 40]. The three types of κ - ϵ model are the Standard κ - ϵ model, RNG κ - ϵ model, and Realizable κ - ϵ model. From these three types of the κ - ϵ turbulent model, Standard κ - ϵ model used in this study because it is suitable to be used with gas-air mixer [1, 24, 34, 40-43]. Robustness, economy and reasonable accuracy for a wide range of turbulent flows of the standard κ - ϵ model in FLUENT explain its popularity in industrial flow and heat transfer simulation [36, 44-46].

The transport equations to obtain the turbulent kinetic energy (k) and its dissipation rate for Standard κ - ϵ model are following [36]

$$\frac{\partial}{\partial t}(\rho k) + \frac{\partial}{\partial x_i}(\rho k u_i) = \frac{\partial}{\partial x_j} \left[\left(\mu + \frac{\mu_t}{\sigma_k} \right) \frac{\partial k}{\partial x_j} \right] + G_k + G_b - \rho \epsilon - Y_M + S_k \quad (2)$$

$$\frac{\partial}{\partial t}(\rho \epsilon) + \frac{\partial}{\partial x_i}(\rho \epsilon u_i) = \frac{\partial}{\partial x_j} \left[\left(\mu + \frac{\mu_t}{\sigma_\epsilon} \right) \frac{\partial \epsilon}{\partial x_j} \right] + C_{1\epsilon} \frac{\epsilon}{k} (G_k + C_{3\epsilon} G_b) - C_{2\epsilon} \rho \frac{\epsilon^2}{k} + S_\epsilon \quad (3)$$

In these equations, G_k Represents the generation of turbulence kinetic energy due to the mean velocity gradients, G_b is the generation of turbulence kinetic energy due to buoyancy. Y_M Is the contribution of the fluctuating dilatation in compressible turbulence to the overall dissipation rate. The quantities α_k and α_ϵ are the inverse effective Prandtl numbers for k and ϵ , respectively. S_k and S_ϵ are user defined source terms [44].

The turbulence intensity for inlet and outlet of mixer can be valued by equation below [1, 36]

$$I \equiv \frac{u'}{u_{avg}} = 0.16 (Re_{D_H})^{-1/8} \quad (4)$$

where Re is Reynolds number, D_H is hydraulic diameter (diameter of inlet section).

3.3.2.3 Mixing flow without reaction

With mixing CNG and air, there is no reaction between air and natural gas and species transport need to be used [14, 24].

3.3.2.4 Species transport

Species transport has been selected because it works effectively with reactions and no reactions between mixed gases [36].

To solve conservation equations for chemical species, ANSYS FLUENT predicts the local mass fraction of each species Y_i , through the solution of a convection-diffusion equation for the i th species. This conservation equation takes the following general form

$$\frac{\partial}{\partial t}(\rho Y_i) + \nabla \cdot (\rho \vec{V} Y_i) = - \nabla \cdot \vec{J}_i + R_i + S_i \quad (5)$$

where R_i is the net rate of production of species i by chemical reaction, and S_i is the rate of creation by adding from the dispersed phase plus any user-defined sources [36].

In turbulent flows, ANSYS FLUENT computes the mass diffusion in the following form

$$\vec{J}_i = -\left(\rho D_{i,m} + \frac{\mu_t}{S_{C_t}}\right) \nabla Y_i - D_{T,i} \frac{\nabla T}{T} \quad (6)$$

where S_{C_t} is the turbulent Schmidt number ($\frac{\mu_t}{\rho D_t}$, where μ_t is the turbulent viscosity, and D_t is the turbulent diffusivity). The default S_{C_t} is 0.7. Note that turbulent diffusion generally overwhelms laminar diffusion, and the specification of detailed laminar diffusion properties in turbulent flows is generally not necessary [36].

The mixture materials that selected in the species transport model are methane-air mixture.

3.3.2.5 Incompressible steady state flow

The fluid flow assumed incompressible flow according to the Mach number which was less than one using Eq. 7 [47]

$$v = Mc \quad (7)$$

where, v is the fluid velocity in meter per second, M is Mach number, and c is the speed of sound in meter per second.

The fluid flow inside the CNG-air mixer is considered a steady state flow [33-35, 40, 48].

3.3.3 Boundary conditions

3.3.3.1 Air inlet

Since the air is sucked into the engine without an external force like supercharger or turbocharger, the air inlet boundary condition was taken as ambient pressure. Table 2 shows the air properties at the air inlet of the mixer. The other values are interpolated from fluid dynamic air properties found in any fluid properties table at the given pressure and temperature.

Table 2

Air properties at the air inlet

Variable	Quantity
Density	1.225 kg/m ³
Temperature	300° k
Dynamic viscosity	0.000017894 kg/ms
Operation pressure	101325 pa

3.3.3.2 Flow rate at the outlet

Target Mass Flow Rate Option was used at the mixer outlet. With this option, the simple Bernoulli's equation is used to adjust the pressure at every iteration on a pressure outlet zone in order to meet the desired mass flow rate. The change in pressure, based on Bernoulli's equation is given by the following equation [36]

$$dP = 0.5\rho_{ave}(\dot{m}^2 - \dot{m}_{req}^2)/(\rho_{ave}A)^2 \quad (8)$$

where dP is the change in pressure, & \dot{m} is the current computed mass flow rate at the pressure-outlet boundary, & \dot{m}_{req} is the required mass flow rate, ρ_{ave} is the computed average density at the pressure outlet boundary, and A is the area of the pressure-outlet boundary.

This target mass flow rate can be calculated by equation below [17]

$$(\dot{m}_a + \dot{m}_g) = \frac{\eta_V \rho_{a,g} V_d^n}{2} \quad (9)$$

where η_V is the volumetric efficiency, $\rho_{a,g}$ (kg/m^3) is the mixing air–gas density, V_d (m^3) is the engine displacement and n (rpm) is the engine speed.

Typical maximum values of volumetric efficiency (η_V) for naturally aspirated engines are in the range between 80% and 90%, and it is for diesel engines somewhat is higher than SI engines [49]. Typical values of volumetric efficiency for an engine at wide-open throttle (WOT) are in the range between 75% and 90%, going down to lower values as the throttle is closed. Restricting air flow into an engine (closing the throttle) is the primary means of power control for a spark ignition engine [50]. For petrol engines, η_V is between 80% and 85 %, whereas for the diesel engine it is in the range 85% to 90% [51]. Therefore, it is assumed as 90% in present work.

Air-gas mixture density can be calculated by Eq. 10 [52, 53]

$$\frac{1}{\rho_{mixture}} = \frac{\frac{m_{gas}}{m_{air}} \times \frac{1}{\rho_{gas}} + \frac{1}{\rho_{air}}}{\frac{m_{gas}}{m_{air}} + 1} \quad (10)$$

3.3.3.3 Methane inlet

In the first test of the mixer, gas pressure assumed as ambient pressure to investigate if the gas can be sucked by high-speed air flow. The second boundary condition is represented by using methane mass flowrate at the methane inlet during pressure investigation and during the test of the mixer with various AFR. This mass flow rate at the methane inlet is calculated by solving Eq. 9, 10, and 11.

$$AFR = \frac{\dot{m}_a}{\dot{m}_f} \quad (11)$$

Table3 summarized methane properties that used in simulation.

Variable	Quantity
Methane density	0.715 kg / m ³
Temperature	300° k
Operation pressure	101325 Pa

4. Results and Discussion

4.1 Air Fuel Ratio and Pressure Investigation

Figure 7 shows methane mass fraction (M_{Ch_4}) at center plane of mixer that there is an insufficient quantity of methane can be sucked to the mixer and air-fuel ratio is equal to 70.11 when the methane inlet pressure was taken as ambient pressure. This high AFR could cause incapability of the engine to combust the air-fuel mixture. Therefore, the gas needs to be supplied with pressure higher than ambient pressure to increase gas mass flowrate and reduce AFR.

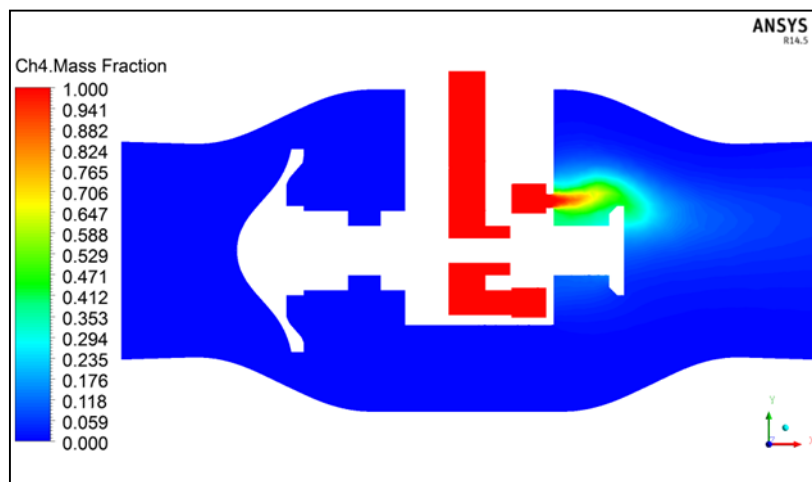


Fig. 7. M_{Ch_4} at the center plane of mixer

The shaft design of control valve closes the gas inlet when it is at the last position with maximum engine speed. The results of CFD showed that the total gauge pressure at the gas inlet should be (2.608 Mpa) to get air-fuel ratio near to stoichiometric ratio (17.2) when the valve at the last position with maximum engine speed (3600 rpm). This pressure is very high and cannot use with the CNG kit since the maximum allowed gas pressure at the pressure regulator is (0.25 Mpa). Figure 8 shows the color contour of total gauge pressure at the center mixer xy plane.

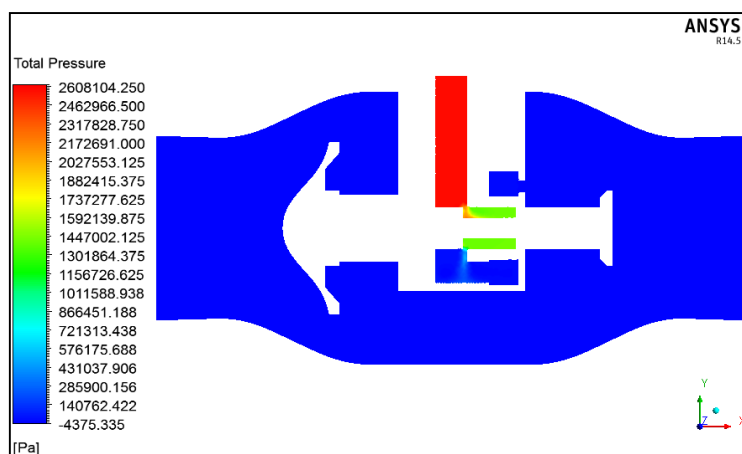


Fig. 8. Total pressure at the XY symmetry plane

In addition to the AFR issue, Figure 9 shows that methane mass fraction (M_{Ch_4}) is accumulated in some regions, especially near to the center axis of the mixer and in the region behind the block of gas manifold.

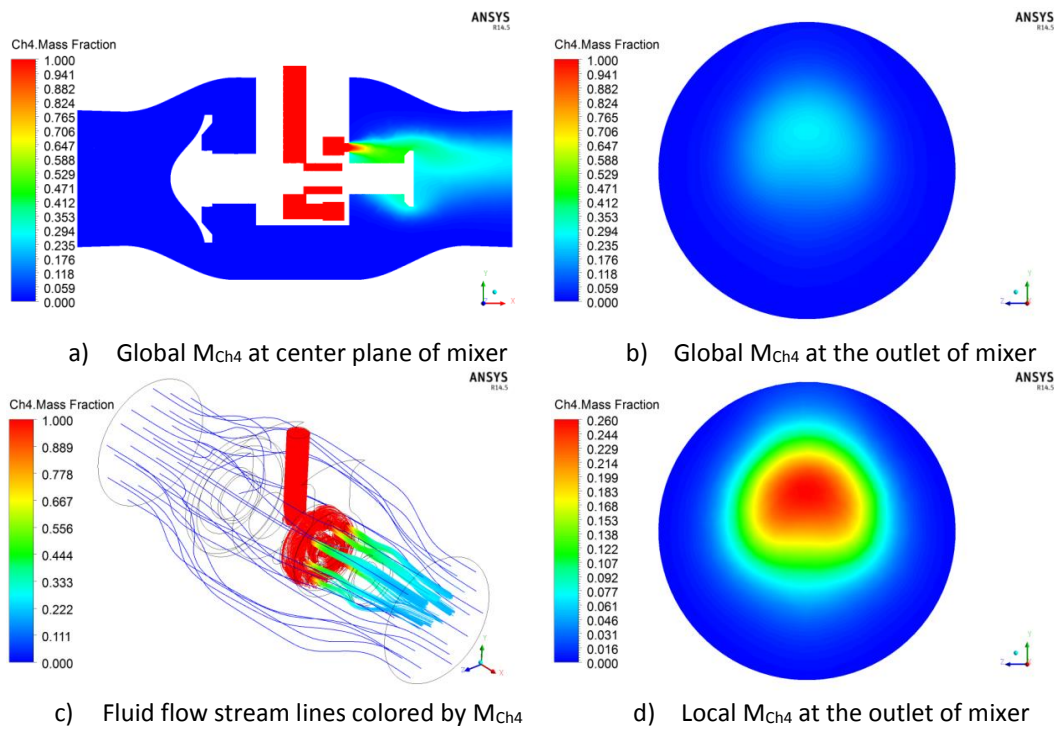


Fig. 9. M_{Ch_4} color contours and fluid flow stream lines

Therefore, the second method which represented by using the maximum allowed pressure (0.25 Mpa) at the gas inlet when the valve was at the last position with maximum engine speed has been used to show the AFR. The results of CFD showed that the AFR is (57.38567388 pa) which is higher than stoichiometric AFR (17.2). Figure 10 shows that methane mass fraction (M_{Ch_4}) is very little and it is accumulated in some regions, especially near the center axis and in the region behind the block of gas manifold. This gas accumulation resulted in a heterogeneous CNG-air mixture.

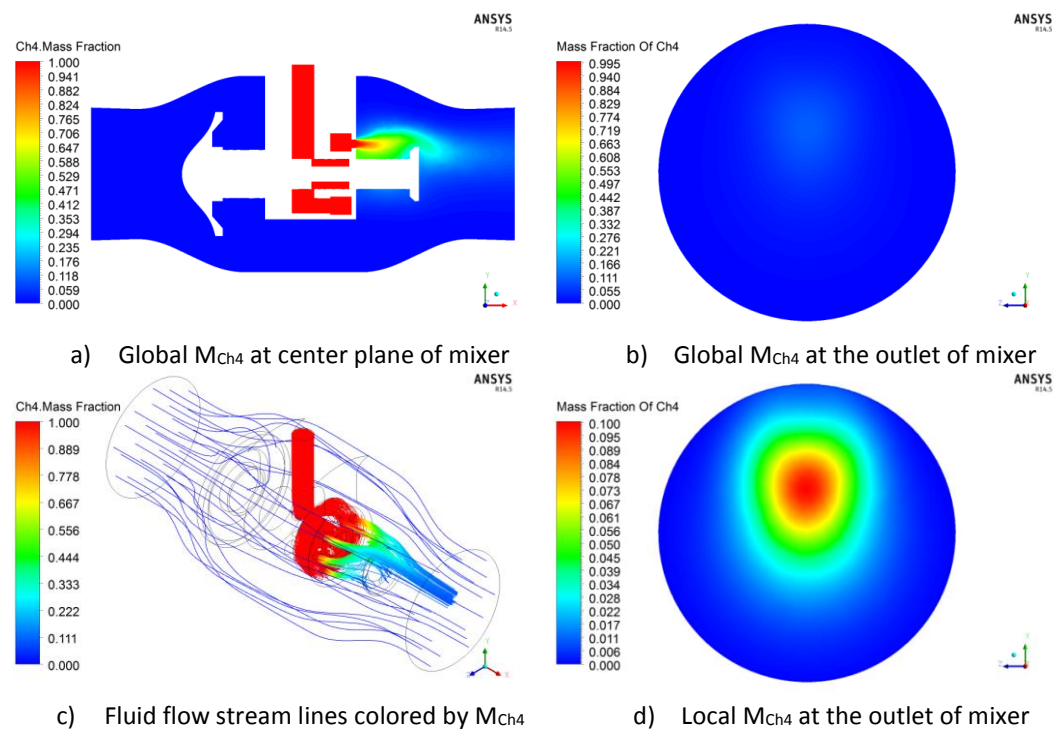


Fig. 10. M_{Ch_4} color contours and fluid flow stream lines

4.2 Testing the Mixer with Various AFR

After testing the mixer with AFR close to stoichiometric ratio, then it was tested with fixed maximum engine speed (3600 rpm) and different AFR (10, 17.2, 20, 30, and 40) to see if the mixer can work properly with other AFR. Maximum engine speed (3600 rpm) was used because the less mixing happens at the maximum engine speed and when the engine speed decreased, the homogeneity increased due to increase the time of mixing. Therefore, if the mixing at the high speed is excellent, of course, the mixing will be better at the other speeds less than maximum speed (trade off relation-Inverse relationship).

CFD test provides several ways to measure the mixture homogeneity either by colors contour, mathematical formulas or values of mass fraction concentration.

For example, the uniformity index γ can be used to estimate the air-fuel mixture homogeneity [25, 36, 54, 55]. The optimum value of the uniformity index γ is equal to 1 [25, 36, 54, 55]. The uniformity index can be weighted by area or mass. Area-weighted uniformity index captures the variation of the quantity, while the mass-weighted uniformity index captures the variation of the flux [36]. The area-weighted uniformity index (γ_a) of a specified field variable ϕ is calculated using Eq. 12 [25, 36, 54, 55]

$$\gamma_a = 1 - \frac{\sum_{i=1}^n [(|\phi_i - \bar{\phi}_a|) A_i]}{2|\bar{\phi}_a| \sum_{i=1}^n A_i} \quad (12)$$

where i is the facet index of a surface with n facets, and $\bar{\phi}_a$ is the average value of the field variable over the surface [36]

$$\bar{\phi}_a = \frac{\sum_{i=1}^n \phi_i A_i}{\sum_{i=1}^n A_i} \quad (13)$$

The color contour is the second method to evaluate the homogeneity of the mixture components. The less number of color contour at the mixing region indicates better mixing. The best mixing happens when the two colors of gas and air merger in one color.

Figure 11 shows the relation between AFR, gas velocity at the gas holes, and uniformity index of methane mass fraction (M_{CH_4}) at the mixer outlet.

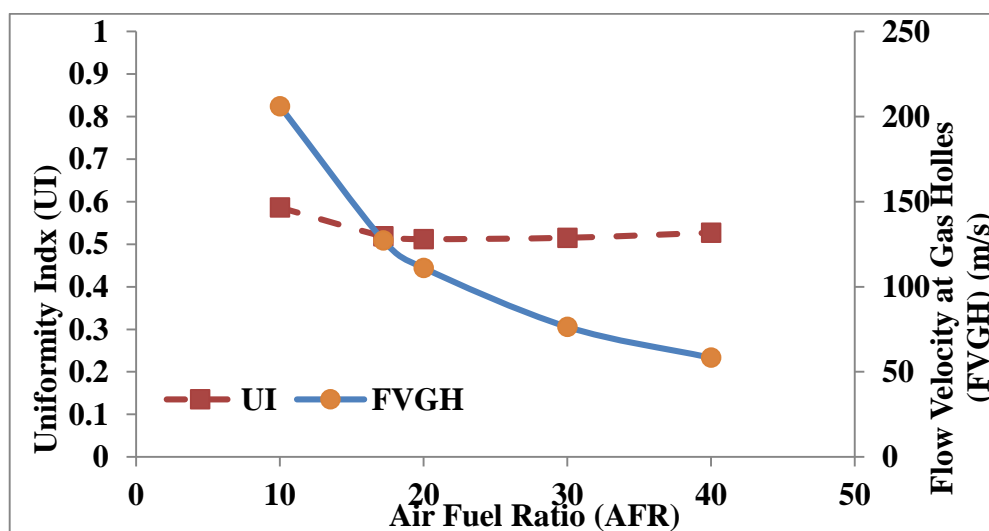


Fig. 11. Relation between AFR, Gas Velocity at the Gas Holes, and UI of M_{CH_4}

From the chart above, it is clear that the methane uniformity index at the mixer outlet is lower than 0.6 with all AFRs. This quantity of UI means that the gas is accumulated in some regions and not uniform on the outlet area as shown in Figure 12.

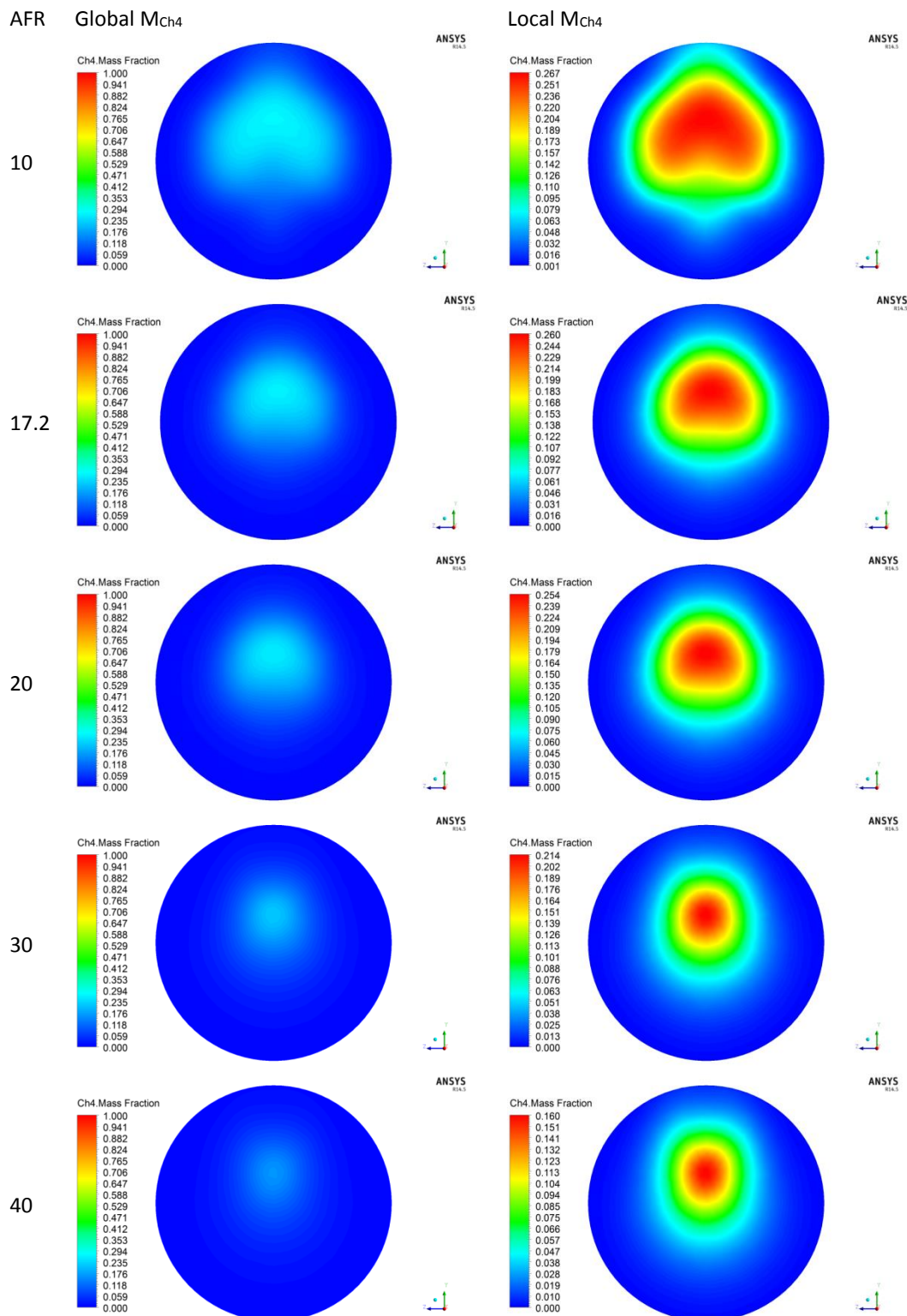


Fig. 12. Global and local M_{Ch_4} color contours at the mixer outlet with various AFRs

5. Conclusions

A commercial CNG–air pre mixing controller mixer for a CNG–diesel dual-fuel engine has been modeled using CATIA and ANSYS design modeler software. The mixer has been simulated using ANSYS Fluent 14.5 software. CFD analysis results showed that the mixer with stoichiometric or other AFR is unable to supply the engine with homogeneous mixture of gas and air. The uniformity index of methane at the mixer outlet is lower than 0.6 with all AFRs. This quantity of UI means that the gas is accumulated in some regions and not uniform on the outlet area. This heterogeneity of CNG and air is related to some factors like mixer internal design, air-fuel ratio, engine speed, control valve position, and gas inlet pressure. Therefore, there is a need to modify the design of this mixer in terms of CNG air mixture homogeneity.

In addition to heterogeneity problem, the mixer is unable to control AFR due to the design of control valve shaft. The air-fuel ratio is equal to 70.11 when the methane inlet pressure was taken as ambient pressure. This high AFR could cause incapability of the engine to combust the air-fuel mixture. Therefore, the gas needs to be supplied with pressure higher than atmospheric pressure to increase gas mass flowrate and reduce AFR. Furthermore, the total gauge pressure at the gas inlet should be (2.608 Mpa) to get air-fuel ratio close to stoichiometric ratio (17.2) when the valve at the last position with maximum engine speed (3600 rpm). This pressure is very high and cannot use with the CNG kit since the maximum allowed gas pressure at the pressure regulator is (0.25 Mpa). Therefore, there is a need to modify the design of this mixer in terms of controlling AFR. At this time, the work is underway to develop the mixer in terms of the air fuel ratio controlling and CNG-air mixture homogeneity.

Acknowledgement

The authors wish to thank Universiti Putra Malaysia for the facilities and The Ministry of Higher Education, Wasit University -Iraq for the financial support of the first author. In addition, this work was also supported by UPM Putra Grant Scheme with Reference Number: GP-IPB-2013-9412900 and was carried out in Universiti Putra Malaysia (UPM). The authors, therefore, would like to record their thanks for the supports.

References

- [1] Chintala, Venkateswarlu, and K. A. Subramanian. "A CFD (computational fluid dynamics) study for optimization of gas injector orientation for performance improvement of a dual-fuel diesel engine." *Energy* 57 (2013): 709-721.
- [2] Taib, Norhidayah Mat, Mohd Radzi Abu Mansor, Wan Mohd Faizal Wan Mahmood, and Nik Rosli. "Simulation study of combustion characteristics of diesel-ethanol-palm oil methyl ester blends in diesel engine." *Journal of Advanced Research in Fluid Mechanics and Thermal Sciences* 44, no. 1 (2018): 149-156.
- [3] Pai, Anand, Vaibhav Kumar Singh, Shailesh Suthar, and Harshit Sharma. "Taguchi Analysis of Combustion of Diesel and Bio-Diesel Blend utilizing Homogeneous Reactor Model." *Journal of Advanced Research in Fluid Mechanics and Thermal Sciences* 52, no. 1 (2018): 94-103.
- [4] Azad, A. K., SM Ameer Uddin, and M. M. Alam. "A comprehensive study of DI diesel engine performance with vegetable oil: an alternative bio-fuel source of energy." *International Journal of Automotive and Mechanical Engineering (IJAME)* 5 (2012): 576-586.
- [5] Lata, D. B., Ashok Misra, and S. Medhekar. "Effect of hydrogen and LPG addition on the efficiency and emissions of a dual fuel diesel engine." *International Journal of Hydrogen Energy* 37, no. 7 (2012): 6084-6096.
- [6] Papagiannakis, R. G., P. N. Kotsiopoulos, T. C. Zannis, E. A. Yfantis, D. T. Hountalas, and C. D. Rakopoulos. "Theoretical study of the effects of engine parameters on performance and emissions of a pilot ignited natural gas diesel engine." *Energy* 35, no. 2 (2010): 1129-1138.
- [7] Wahbi, A., A. Tsolakis, and J. Herreros. "Emissions Control Technologies for Natural Gas Engines." In *Natural Gas Engines*, pp. 359-379. Springer, Singapore, 2019.

- [8] Shaikh, M. A., and Aditya H. Shukla. "Optimization of natural gas mixture design by computational method for improving swirl effect to obtain enhancement of SI engine performance: A Review." *International Journal of Current Engineering and Technology* 6, no.5 (2016).
- [9] Kamil, Mohammed, M. M. Rahman, and Rosli A. Bakar. "Performance evaluation of external mixture formation strategy in hydrogen fueled engine." *Journal of Mechanical Engineering and Sciences* 1 (2011): 87-98.
- [10] Yusaf, Talal F., D. R. Buttsworth, Khalid H. Saleh, and B. F. Yousif. "CNG-diesel engine performance and exhaust emission analysis with the aid of artificial neural network." *Applied Energy* 87, no. 5 (2010): 1661-1669.
- [11] Dahake, M., S. Patil, and S. Patil. "Performance and Emission Improvement through Optimization of Venturi Type Gas Mixer for CNG Engines." *Int. Res. J. Eng. Technol* 3 (2016): 994-999.
- [12] Mahla, Sunil Kumar, and Amit Dhir. "Performance and emission characteristics of CNG-fueled compression ignition engine with Ricinus communis methyl ester as pilot fuel." *Environmental Science and Pollution Research* 26, no. 1 (2019): 975-985.
- [13] Mattson, Jonathan MS, Chenaniah Langness, and Christopher Depcik. *An analysis of dual-fuel combustion of diesel with compressed natural gas in a single-cylinder engine*. No. 2018-01-0248. SAE Technical Paper, 2018.
- [14] Yusaf, T., P. Baker, I. Hamawand, and M. M. Noor. "Effect of compressed natural gas mixing on the engine performance and emissions." *International Journal of Automotive and Mechanical Engineering* 8, no. 1 (2013): 1416-1429.
- [15] Talekar, Apoorv, Ming-Chia Lai, Eiji Tomita, Nobuyuki Kawahara, Ke Zeng, and Bo Yang. *Numerical Investigation of Natural Gas-Diesel Dual Fuel Engine with End Gas Ignition*. No. 2018-01-0199. SAE Technical Paper, 2018.
- [16] Kapilan, N., T. P. Ashok Babu, and R. P. Reddy. "Improvement of performance of dual fuel engine operated at part load." *International Journal of Automotive and Mechanical Engineering* 2 (2010): 200-10.
- [17] Bedoya, Ivan Dario, Andres Amell Arrieta, and Francisco Javier Cadavid. "Effects of mixing system and pilot fuel quality on diesel-biogas dual fuel engine performance." *Bioresource technology* 100, no. 24 (2009): 6624-6629.
- [18] Khan, Muhammad Imran, Tabassum Yasmin, and Abdul Shakoor. "Technical overview of compressed natural gas (CNG) as a transportation fuel." *Renewable and Sustainable Energy Reviews* 51 (2015): 785-797.
- [19] Chang, YS, Z Yaacob, and R Mohsin. "Computational Fluid Dynamics Simulation of Injection Mixer for CNG Engines." Paper presented at the Proceedings of the World Congress on Engineering and Computer Science (WCECS 2007), San Francisco, CA, USA, 2007.
- [20] Noor, M. M., K. Kadirgama, R. Devarajan, M. R. M. Rejab, N. M. Zuki, and Talal Yusaf. "Development of a high pressure compressed natural gas mixer for a 1.5 litre CNG-diesel dual engine." In *Proceedings of the National Conference on Design and Concurrent Engineering (DECON) 2008*, pp. 435-438. Universiti Teknikal Malaysia Melaka, 2008.
- [21] Vongsateanchai, Supoj, Cholathorn Rakdee, Wisoth Vainaisompan, and Nitnipa Seanglum. Secondary Fuel Premixing Controller for an Air Intake Manifold of a Combustion Engine. US 2011.
- [22] Prakash, R. Paullinga, S. Palani, D. Vijaya Kumar, S. Arun Kumar, and S. Shanmugam. "Flow Behaviour Analysis of Injection Mixer for CNG Engines using Computational Fluid Dynamics." *International Journal of Vehicle Structures & Systems* 9, no. 5 (2017): 284-287.
- [23] Supee, A., M. S. Shafeez, R. Mohsin, and Z. A. Majid. "Performance of diesel-compressed natural gas (CNG) dual fuel (DDF) engine via CNG-air venturi mixjector application." *Arabian Journal for Science and Engineering* 39, no. 10 (2014): 7335-7344.
- [24] Gorjibandpy, Mofid, and Mehdi Kazemi Sangsereki. "Computational investigation of air-gas venturi mixer for powered bi-fuel diesel engine." *World Academy of Science, Engineering and Technology* 4, no. 11 (2010): 1197-1201.
- [25] Abo-Serie, Essam, M. Özgür, and K. Altinsik. "Computational analysis of methane-air venturi mixer for optimum design." In *Proceedings of the 13th International Combustion Symposium, Bursa, Turkey*, pp. 9-11. 2015.
- [26] Yusaf, Talal, and Mohammed Zamri Yusoff. "Development of a 3D CFD model to investigate the effect of the mixing quality on the CNG-diesel engine performance." In *Proceedings of the International Conference and Exhibition and Natural Gas Vehicles*. IANGV International Association of Natural Gas Vehicles, 2000.
- [27] Abagnale, Carmelina, Maria Cristina Cameretti, Luigi De Simio, Michele Gambino, Sabatino Iannaccone, and Raffaele Tuccillo. "Combined numerical-experimental study of dual fuel diesel engine." *Energy procedia* 45 (2014): 721-730.
- [28] Badr, O., G. A. Karim, and B. Liu. "An examination of the flame spread limits in a dual fuel engine." *Applied Thermal Engineering* 19, no. 10 (1999): 1071-1080.
- [29] Karim, G. A., and M. O. Khan. "Examination of effective rates of combustion heat release in a dual-fuel engine." *Journal of Mechanical Engineering Science* 10, no. 1 (1968): 13-23.

- [30] Papagiannakis, R. G., and D. T. Hountalas. "Experimental investigation concerning the effect of natural gas percentage on performance and emissions of a DI dual fuel diesel engine." *Applied Thermal Engineering* 23, no. 3 (2003): 353-365.
- [31] Papagiannakis, R. G., and D. T. Hountalas. "Combustion and exhaust emission characteristics of a dual fuel compression ignition engine operated with pilot diesel fuel and natural gas." *Energy conversion and management* 45, no. 18-19 (2004): 2971-2987.
- [32] Sahoo, B. B., N. Sahoo, and U. K. Saha. "Effect of engine parameters and type of gaseous fuel on the performance of dual-fuel gas diesel engines—A critical review." *Renewable and Sustainable Energy Reviews* 13, no. 6-7 (2009): 1151-1184.
- [33] Ramasamy, Devarajan. "Development of a Compressed Natural Gas (CNG) Mixer for a Two Stroke Internal Combustion Engine." PhD diss., Universiti Teknologi Malaysia, 2006.
- [34] Danardono, Dominicus, Ki-Seong Kim, Sun-Youp Lee, and Jang-Hee Lee. "Optimization the design of venturi gas mixer for syngas engine using three-dimensional CFD modeling." *Journal of mechanical science and technology* 25, no. 9 (2011): 2285-2296.
- [35] De Castro, Jônathas Assunção SN, Taygoara Felamino de Oliveira, and Carlos Humberto Llanos Quintero. "Numerical analysis and optimization of mixers." (2012).
- [36] Fluent, A. N. S. Y. S. "14.0. Documentation, ANSYS Inc. Canonsburg, PA, USA." (2012).
- [37] Bergman, T. L., A. S. Lavine, F. P. Incropera, and D. P. Dewitt. "Fundamentals of Happel, John, and Howard Brenner. Low Reynolds Number Hydrodynamics: With Special Applications to Particulate Media. Vol. 1: Springer Science & Business Media, 2012.
- [38] Happel, John, and Howard Brenner. *Low Reynolds number hydrodynamics: with special applications to particulate media*. Vol. 1. Springer Science & Business Media, 2012.
- [39] Wei, Ong Yong, and siti ujila masuri. "Computational Fluid Dynamics Analysis on Single Leak and Double Leaks Subsea Pipeline Leakage." *Signal* 11, no. 2 (2019): 95-107.
- [40] Anil, T. R., S. D. Ravi, M. Shashikanth, P. G. Tewari, and N. K. S. Rajan. "CFD analysis of a mixture flow in a producer gas carburetor." In *International Conference On Computational Fluid Dynamics, Acoustics, Heat Transfer and Electromagnetics CFEMATCON-06*. 2006.
- [41] Reddy, Raj, and Pooja Reddy. "Analysis of producer gas carburetor for different air-fuel ratios using CFD." *International Journal of Research in Engineering and Technology* 3 (2014): 470-474.
- [42] Yeap, Beng Hi, Azeman Mustafa, and Zulkefli Yaacob. "Computational Investigation of Air-Fuel Mixing System for Natural Gas Powered Motorcycle." Paper presented at the Proceedings of the 15th Symposium of Malaysian Chemical Engineers SOMChE 2001, 2001.
- [43] Sharma, Harshwardhan, Satyendra Singh, and Ravi Goel. "CFD analysis of the natural gas based Carburetor for a two stroke spark Ignition engine." In *Research paper, National Conference on "Recent Advances in Mechanical Engineering*. 2014.
- [44] Coffield, David, and Doug Shepherd. "Tutorial guide to Unix sockets for network communications." *Computer Communications* 10, no. 1 (1987): 21-29.
- [45] Geankopolis, Christie J. *Transport processes and unit operations*. Prentice-Hall, 1993.
- [46] Srinivas, Karkenahalli, and Clive Fletcher. *Computational techniques for fluid dynamics: a solutions manual*. Springer Science & Business Media, 2002.
- [47] Kadirgama, K., M. M. Noor, A. R. N. A. Rahim, R. Devarajan, M. R. M. Rejab, and NM Zuki NM. "Design and Simulate Mixing of Compressed Natural Gas with Air in a mixing device." In *Proceedings of the MUCET2008, Malaysian Technical Universities Conference on Engineering and Technology, Putra Palace, Perlis, Malaysia*, pp. 15-16. 2008.
- [48] Sera, Mardani Ali. "Development of intake system for improvement of performance of compressed natural gas spark ignition engine." PhD diss., Universiti Teknologi Malaysia, 2004.
- [49] Heywood, John B. "Internal Combustion Engine Fundamentals, Vol. 930mcgraw-Hill." New York (1988).
- [50] Pulkrabek, Willard W. *Engineering fundamentals of the internal combustion engine*. No. 621.43 P8. 1997.
- [51] Kumar, Devender, Sumeet Guide Sharma, and D. Gangacharyulu. "Studies on improvement of intake manifold for compressed natural gas engine." PhD diss., 2012.
- [52] Guibet, Jean-Claude. "Fuels and Engines-Technology, Energy and Environment, Vol. 1 & 2." Technip, Paris, latest edition (1997).
- [53] Jemni, M. A., G. Kantchev, and M. S. Abid. "Intake manifold design effect on air fuel mixing and flow for an LPG heavy duty engine." *International journal of energy and environment* 3, no. 1 (2012): 61-72.
- [54] Kim, J. N., Ho Young Kim, S. S. Yoon, and S. D. Sa. "Effect of intake valve swirl on fuel-gas mixing and subsequent combustion in a CAI engine." *International journal of automotive technology* 9, no. 6 (2008): 649-657.
- [55] Weltens, Herman, Harald Bressler, Frank Terres, Hubert Neumaier, and Detlev Rammoser. *Optimisation of catalytic converter gas flow distribution by CFD prediction*. No. 930780. SAE Technical Paper, 1993.